

# **Axial and Lateral Small Strain Measurement of Soils in Compression Test using Local Deformation Transducer**

Hasbullah Nawir<sup>1,2,\*</sup>, Dayu Apoji<sup>2</sup>, Riska Ekawita<sup>3</sup> & Khairurrijal Khairurrijal<sup>4</sup>

Abstract. This paper presents the development of a method using local deformation transducers (LDTs) to locally and sensitively measure small axial and lateral strains in soil in a compression test. A local strain measurement system comprising of axial and lateral LDTs was developed referring to the original LDT system and the cantilever LDT system, respectively. The LDTs were calibrated both in air and under water. Their insensitivity to pressurized water was confirmed. The calibration factors for the axial and lateral LDTs were found to be 1.695 mm/volt and 1.001 mm/volt, respectively. The performance in terms of repeatability and stability of the LDT system was evaluated. The repeatability test showed that the average standard deviation of the lateral LDT was 0.015 volt, while the stability test showed that the average standard error of the axial and lateral LDT were  $3.13 \times 10^{-5}$  volt and  $2.65 \times 10^{-5}$  volt, respectively. Unconfined compression tests were conducted on three reconstituted clay samples to examine the proposed axial and lateral LDT system. The stress-strain relationship indicates a nonlinear relationship between the axial and lateral strain of soil instead of the conventionally assumed constant relationship. The results demonstrate this nonlinear behavior even at small strain levels, which were successfully measured using a domestically built axial and lateral LDT system.

**Keywords:** axial strain; lateral strain; local deformation transducer; nonlinear behavior; small strain measurement; unconfined compression test.

#### 1 Introduction

It has been reported that external strain measurements of soil specimen deformation (i.e. measurements of axial deformation of the specimen outside the triaxial cell or at the specimen cap) may seriously underestimate the true stiffness for various types of stiff soils [1] and soft rocks [2]. This error can

Received April 18<sup>th</sup>, 2017, 1<sup>st</sup> Revision November 2<sup>nd</sup>, 2017, 2<sup>nd</sup> Revision December 27<sup>th</sup>, 2017, Accepted for publication February 28<sup>th</sup>, 2018.

Copyright ©2018 Published by ITB Journal Publisher, ISSN: 2337-5779, DOI: 10.5614/j.eng.technol.sci.2018.50.1.4

occur because of: (i) system compliance (e.g. deflection of cell pressure, top cap, loading piston, etc.); (ii) tilting of the specimen; (iii) bedding errors at the top and bottom of the specimen; and (iv) strain non-uniformity of the specimen, including shear bending [3]. Local strain measurement by direct contact between the strain gauge and the soil specimen, unlike external strain measurement, can produce a more reliable result.

Several devices that locally and sensitively measure strain in a triaxial test have been developed in the last three decades to understand the small-strain behavior of soil. Up to now, several types of local strain gauges have been developed, including: (i) electrolytic level gauge [4]; (ii) Hall effect semiconductor [5,6]: (iii) proximity transducer [7]; (iv) local deformation transducer (LDT) [3,8]; and (v) linear variable differential transformer (LVDT) [9,10]. Other methods, such as image processing, have also been developed [11,12]. A comprehensive review of local deformation measurement systems for triaxial tests has been reported by Yimsiri and Soga [13].

The selection of a local deformation measurement system is often made based on cost effectiveness. Among the available systems, LDT is considered to be one of the most low-cost devices [8]. The original LDT system was developed by Goto, *et al.* [3] based on the theory of elasticity for hinged thin columns subject to axial force. Subsequently, Yimsiri, *et al.* [8] modified it to a cantilever-type LDT system, where the transducer behaves as a cantilever beam and the deflection at its free end is measured by the output from the strain gauges attached near the fixed end. The local axial strain is obtained from the relative movements of two cantilever LDTs. Although the cantilever type LDT has lower sensitivity, it has several advantages compared to the original LDT. For instance: (i) it exhibits a linear calibration curve; (ii) it is capable of releasing itself at large strains; and (iii) it has a larger working range [8]. Recently, a pin type LDT has been developed to comply with shear deformation of hollow cylindrical specimens under torsional loading [14,15].

Despite the continuous development of LDT systems, most previous studies focused on the measurement of the axial strain of the specimen [3,8,16]. It is important to note that the deformation of a triaxial test specimen takes place not only in its axial direction but also in its lateral direction. Consequently, local sensitive measurement of both axial and lateral strain is required to accurately evaluate the stress-strain behavior of triaxial test specimens and strain paths in terms of volumetric and shear strain exhibited by the specimen. A cantilever type local lateral strain gauge has been developed by Tatsuoka, *et al.* [17]. A lateral LDT system has also been applied successfully on a large cubical specimen [18-21]. Nevertheless, only a limited number of studies discuss this type of deformation in cylindrical soil specimens [22].

Furthermore, although LDT has been developed and used widely by other researchers globally, it has not been applied prevalently Indonesia, where only few researches on the topic of experimental soil mechanics and small strain measurement of soils have been conducted. Despite having a huge land area and innumerable types of soils, only a limited number of studies have been comprehensively performed to characterize these materials, especially their small strain behaviors.

In this study, an LDT system was developed to locally measure axial and lateral deformations of cylindrical soil specimens in unconfined compression tests. The axial LDT was developed according to the original LDT [3], while the lateral LDT was developed based on the cantilever type LDT [8,17]. The LDTs were calibrated both in air and under water inside a triaxial cell. Their insensitivity to pressurized water was confirmed. The proposed system was then validated by repeatability and stability tests. Subsequently, unconfined compression tests were conducted on three clay samples to evaluate the performance of the proposed LDT system.

This study is part of a development program on experimental soil mechanics that is currently being piloted at the Soil Mechanics Laboratory, Institut Teknologi Bandung. The objectives of this study are: (i) to demonstrate the development of a domestically built LDT system in Indonesia; (ii) to establish an integrated axial and lateral measurement system for soil using LDTs; and (iii) to validate the developed LDT system in 'basic' compression testing before implementing it in more comprehensive soil testing in future experiments.

# 2 Theory of Axial and Lateral LDTs

#### 2.1 Deformation of Axial LDT

An axial LDT is attached to the lateral face of the specimen and allowed to bend according to the specimen's axial deformation during the compression (or shearing) stage. In this system, the measured strain (i.e. output voltage) of the LDT is considered the axial strain of the specimen. The theoretical background of the relationship between gauge strain and axial strain has been discussed by Goto, *et al.* [3] and is briefly presented in this section.

As mentioned above, the concept of axial LDT is based on the theory of elasticity for a hinged thin column subjected to axial force [3]. Figure 1 shows an LDT strip with the axial direction arranged on the x axis and bent toward the y axis.

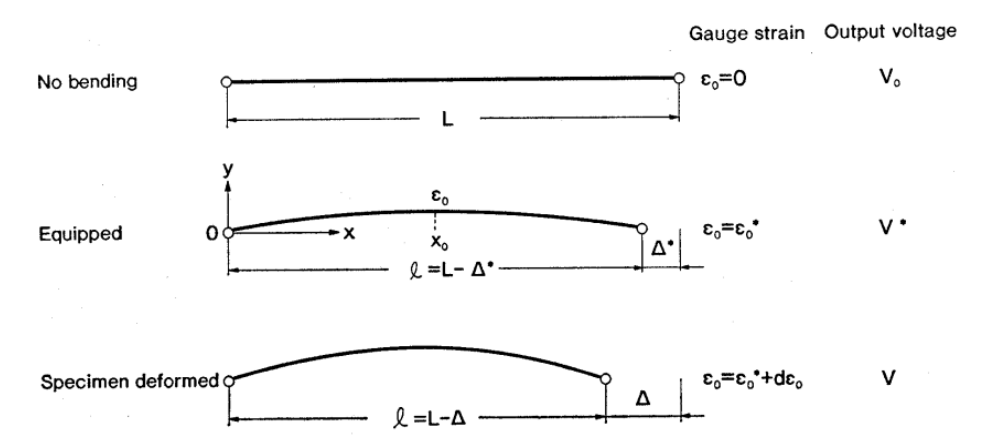


Figure 1 Deformation mode of axial LDT (taken from [3]).

The LDT's length (L) can be calculated from a definite integral of a region from x = 0 to x = L. By defining the length of the deformed LDT as l, the relative deformation  $(\Delta)$  is given in Eq. (1) as follow:

$$\Delta = L - l = \int_0^L \sqrt{1 + \left(\frac{dy}{dx}\right)^2 dx} - l \tag{1}$$

Applying a polynomial series and assuming that the plate's deformation is  $y = a \cdot sin(\pi x/l)$ , where a is a coefficient, the relative deformation can be further derived as in Eq. (2) below:

$$\Delta = \frac{1}{2} \frac{a^2 \pi^2}{l^2} \int_0^l \left[ \frac{1 + \cos(\frac{2\pi x}{l})}{2} \right] dx = \frac{(a\pi)^2}{4l}$$
 (2)

This equation can also be stated in another form expressed in Eq. (3):

$$a = \frac{2\sqrt{\Delta_t \, l}}{\pi} \tag{3}$$

Using the general theory of the bending moment of a deflected plate,  $M = -EI(d^2y/dx^2)$ , the bending moment at the original point of  $x_0$  can be expressed as:

$$M_0 = EI\left(a\frac{\pi^2}{dl^2}sin\left(\frac{\pi x_0}{l}\right)\right) \tag{4}$$

Eq. (4) can be substituted into the theoretical stress and bending moment relationship,  $\sigma = Mt/2I$ . In this case, the stress can be expressed in Eq. (5) as:

$$\sigma_0 = \frac{-EI\left(-a\frac{\pi^2}{dl^2}sin\left(\frac{\pi x_0}{l}\right)\right)t}{2I} \tag{5}$$

where t is plate thickness and I is moment of inertia.

Further, by substituting coefficient a into this equation, the stress can be expressed in Eq. (6) as:

$$\sigma_0 = \frac{E\pi}{l} \sqrt{\frac{\Delta}{l}} \cdot t \cdot \sin\left(\frac{\pi x_0}{l}\right) \tag{6}$$

Using Hook's stress-strain relationship of  $\varepsilon_0 = \sigma_0/E$  and substituting Equation 6 into this equation, the strain and deformation relationship can be determined in Eq. (7) as follows:

$$\Delta = \frac{l^3}{(\pi t)^2} \varepsilon_0^2 \tag{7}$$

Figure 2 shows the elastic bending of the LDT material in detail. The ABCD plane denotes the region of the LDT that undergoes bending deformation. Resistance-wire strain gauges should be located inside this region to measure the deformation accurately. In bending deformation, the AC region and BD region receive inversely proportional forces. For example, the BD region is stretched when the AC region is contracted. The sum of all moments acting on the plane is referred to as the bending moment. In this study, a resistance wire strain gauge was fixed inside the AC region.

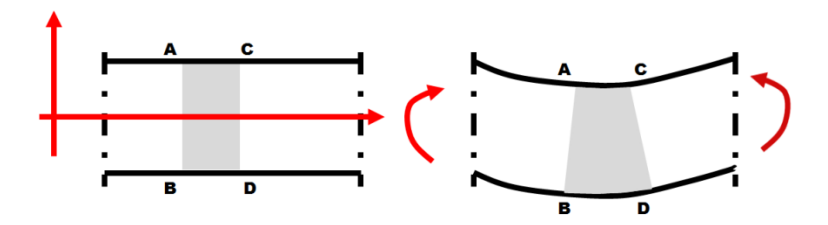


Figure 2 Elastic bending of LDT material.

#### 2.2 Deformation of Lateral LDT

Figure 3 shows the deformation mode of the lateral LDT. One tip of the LDT strip is fixed to a cantilever beam and the other tip is allowed to move following the lateral displacement of the specimens. The strip deformation is assumed to be taking place only in this lateral displacement (y). The axial deformation of the LDT strip is envisaged to be insignificant and thus can be neglected. Using the same stress and bending moment theory as in the previous case, the relationship between lateral strain  $(\varepsilon_r)$  and lateral deformation is given in Eq.  $(\varepsilon_r)$  as follow:

$$y = -\frac{2 \varepsilon_r L^2}{3t} \tag{8}$$

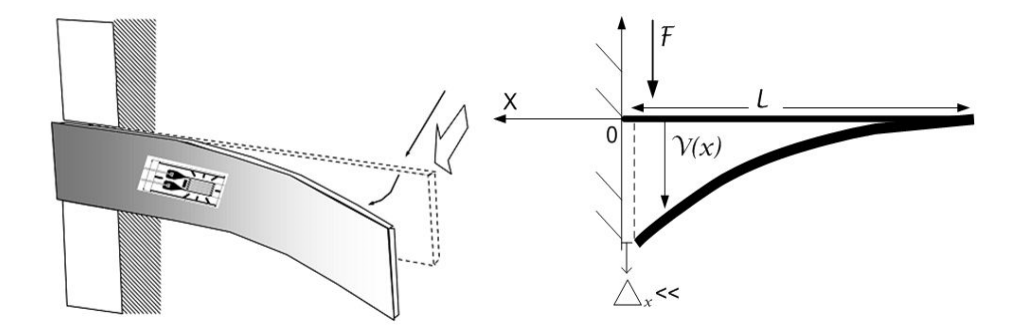


Figure 3 Deformation mode of the lateral LDT.

## 3 Setup

#### 3.1 LDT Device

An LDT device is composed of a thin rectangular strip of linear elastic material with resistance-wire strain gauges attached to its sides. Commonly, the material is selected to comply with the type of the proposed resistance-wire strain gauge. In this study, the LDTs were made of thin rectangular strip of copper beryllium (CuBe) with modulus elasticity equal to 131 kN/mm². The lengths of the axial and the lateral LDT strips were 50 mm and 35 mm, respectively. Width and thickness of both axial and lateral LDT strips were 50 mm and 0.2 mm, respectively. These dimensions were selected to comply with the dimensions of the clay specimens used in the compression test (i.e. 38.1 mm diameter and 76.2 mm height). The dimensions of the LDT could be varied depending on the size and shape of the specimens.

Unlike in the previous study, only a single resistance-wire strain gauge was attached to each LDT strip. This approach was considered to simplify the LDT design and further reduce the cost. The resistance-wire strain gauge used in this study was KFG-5-120-C1-16L1M2R (Kyowa Electronic Instruments Co. Ltd., Japan) with a gauge factor of 2.1  $\Omega$  and a gauge resistance of 119.6±0.4  $\Omega$ . For the axial LDT, the single resistance-wire strain gauge was attached to the center of the LDT strip. For the lateral LDT, the single resistance-wire strain gauge was attached at 5 mm from the edge of each of the four LDT strips. CC-33A adhesive and a waterproof seal (Kyowa Electronic Instruments Co. Ltd.) were used to bond the resistance-wire strain gauge to the LDT strip.

## 3.2 Compression Test Apparatus and LDT System

Unconfined compression tests were performed in this study to examine the axial and lateral deformation measurement of soil specimens using the proposed LDT system. The unconfined compression tests were carried out using a triaxial test apparatus (ELE International Ltd.). The compression test was performed under confined conditions as the basic compression conditions in [23,24] before the proposed system was further subjected to a more multifaceted test under the triaxial conditions in the subsequent study [25]. To measure the deformation of the specimen in the axial and lateral directions during shearing, the specimen was instrumented with a single axial LDT and four lateral LDTs, as shown in the schematic illustration in Figure 4.

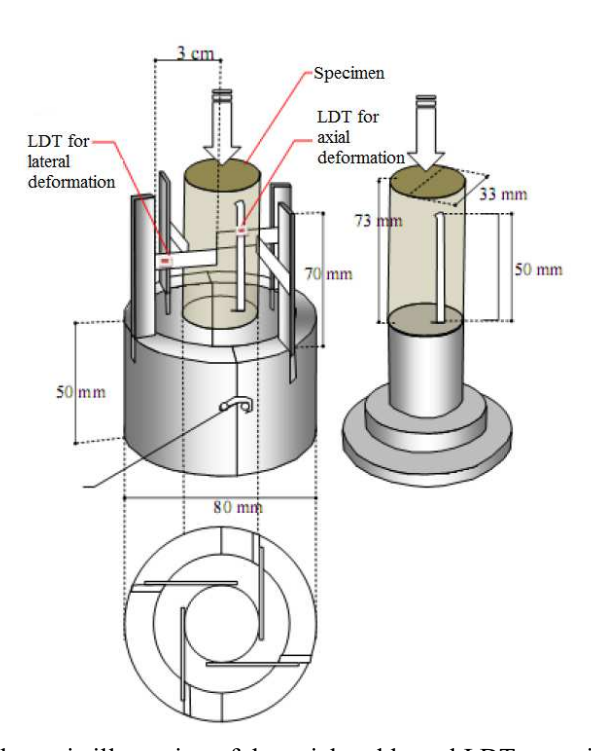


**Figure 4** Schematic illustration of the axial and lateral LDT setup in the triaxial test (taken from [14]).

Following the original LDT setup described by Goto, *et al.* [3], an axial LDT was attached to the membrane in the longitudinal direction of the specimen. A single axial LDT was considered sufficient for this test since no significant eccentricity in the axial loading system was observed from a previous compression test using a rubber dummy specimen [27]. In that study, three axial LDTs attached to the dummy specimen produced comparable measurements. It

would be more recommended to use a pair of axial LDTs arranged at the opposite ends of the specimen diameter to compensate for errors due to inevitable inclination of the specimen axis upon axial loading. In this study, however, only a single axial LDT was used due to limited available space. The use of a pair of axial LDTs in a compression test will be performed after acceptable performance of the single axial LDT has been confirmed.

As shown in Figure 5, the lateral LDT strip was fastened between a rectangular metal piece and a cantilever metal beam of 80 mm height, 10 mm width, and 3 mm thickness to secure the LDT's position. The bottom of each cantilever beam was attached to the top of an aluminum cylinder of 50 mm height, 80 mm diameter, and 10 mm thickness.

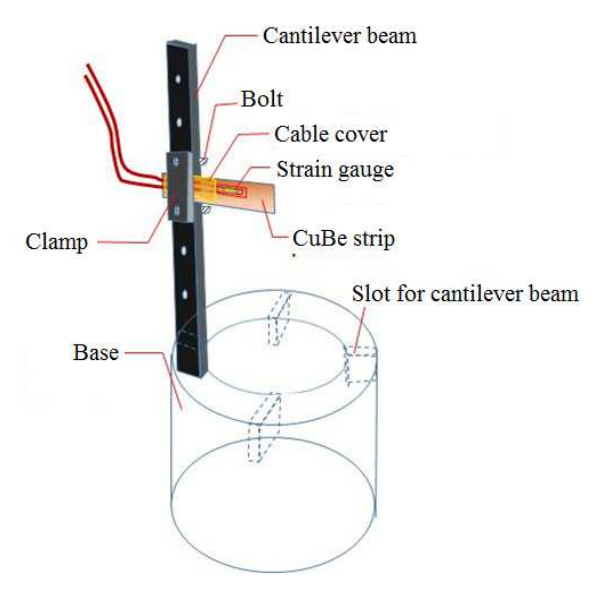


Figure 5 Arrangement of the lateral LDT.

## 3.3 Electronical System

The electronical system is one of the key elements in LDT-based small strain measurement [28]. In this study, each of the developed LDTs was connected to a Wheatstone bridge system, as shown in Figure 6. The Wheatstone bridge system comprised of an LDT device, two resistors of 120  $\Omega$  and a variable resistor. The system was powered by a 3.3-volt VCC from a LM3940 regulator that was used to stabilize the VCC voltage. This Wheatstone bridge enabled the strain measurement by converting the resistance alteration due to LDT strip deformation to an output voltage. To avoid influence of ambient temperature

changes on the system and its output, the laboratory temperature was kept constant at 25° C during the experiment.

An IC multiplexer 4051 was assembled to the Wheatstone bridge to read the system's voltage. Subsequently, the voltage readings were amplified using an AD620 instrument amplifier (Figure 7). This amplifier is a closed-loop amplifier comprised of several operational amplifiers. In this system, the input differential and the amplification magnitude can be adjusted based on the value of external resistor R2. Following the signal amplification, a 16 bits A/D converter of ADS8509 (Texas Instruments Inc.) with an input voltage of 0-3.3 volt was used to convert the analog readings to digital signals. The resolution of the logging system was  $5 \times 10^{-5}$  volt. The digital signals were then forwarded to a microcontroller that was connected to a computer. The data acquisition was carried out by processing the data in the microcontroller using a computer program.

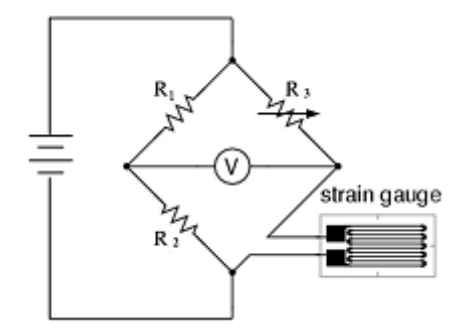


Figure 6 Wheatstone bridge arrangement.

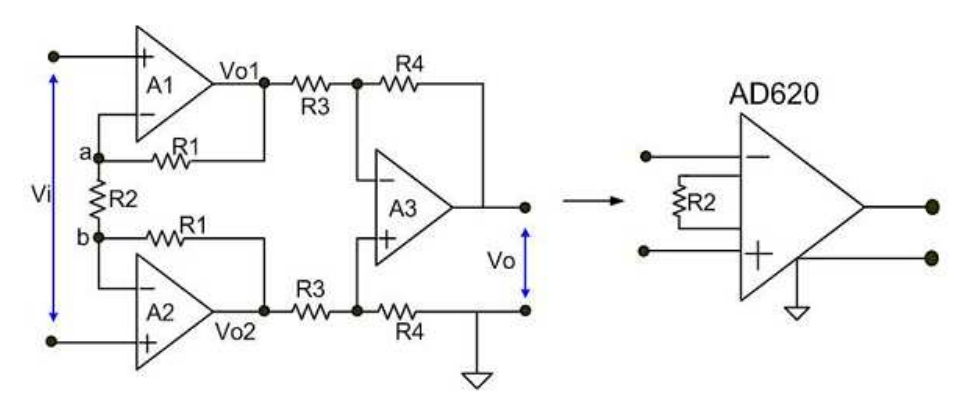
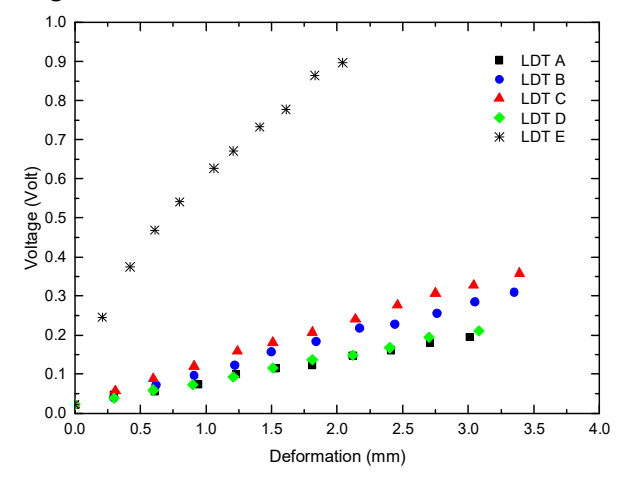


Figure 7 Schematic diagram of instrument amplifier AD620.

#### 4 Calibration

Calibration of the LDTs was performed to determine the relationship between the LDT deformation and the corresponding produced signal. In this calibration, the LDTs were forced to deform over a particular distance (in mm). At a specified distance increment, the signal (i.e. output voltage) as a response to the deformation was measured. Figure 8 shows the calibration result of the lateral LDTs (A, B, C, D) and the axial LDT (E). As can be seen in this figure, the axial LDT produced a nonlinear relationship between the deformation and the output voltage. Having a system similar to the original LDT, this result complies to the calibration curve produced by Goto, *et al.* [3]. In contrast, essentially linear curves were produced by the lateral LDTs up to the considered working range of 3 mm. These results are in accordance with the calibration curve of the cantilever-LDT produced by Yimsiri, *et al.* [8]. These results are reasonable since the deformation mechanisms of the lateral LDT were similar to those of the cantilever LDT (free movement only at one end of the LDT strip).

The calibration was performed both inside and outside the water to evaluate the sensitivity of the LDT performance toward the cell water in the triaxial cell. In this study it was observed that the average voltage response differences produced by the LDT calibration inside and outside the water were about 0.022 volt (for the axial LDT) and 0.021 volt (for the lateral LDT). It was determined that the average secant calibration factor for the axial LDT for a range of deformation between 0 to 1.0 mm was 1.695 mm/volt (voltage change of 0.59 volt for every 1 mm LDT deformation). Note that the non-linear function fitted to the relation shown in Figure 9 was used to obtain the axial deformation for each output voltage from the axial LDT.



**Figure 8** Relationship between LDT deformation (mm) and voltage (V) of the lateral LDTs (A, B, C, D) and the axial LDT (E).

It was also determined that the calibration factor for the lateral LDTs was 10.01 mm/volt (voltage change of 0.0999 volt for every 1 mm LDT deformation). The data obtained from the calibration were then processed to produce their deformation-related resistance value. The relationship between LDT deformation (mm) and resistance change of the resistance-wire strain gauge ( $\Omega$ ) is shown in Figure 9. A linear relationship was produced with all the lateral LDTs, while the relationship was noticeably non-linear with the axial LDT. It can be observed that this relationship was inversely proportional, where a greater deformation of the LDT resulted in a smaller resistance of the strain gauge. This result has been highlighted in a previous study by Ekawita, *et al.* [26].

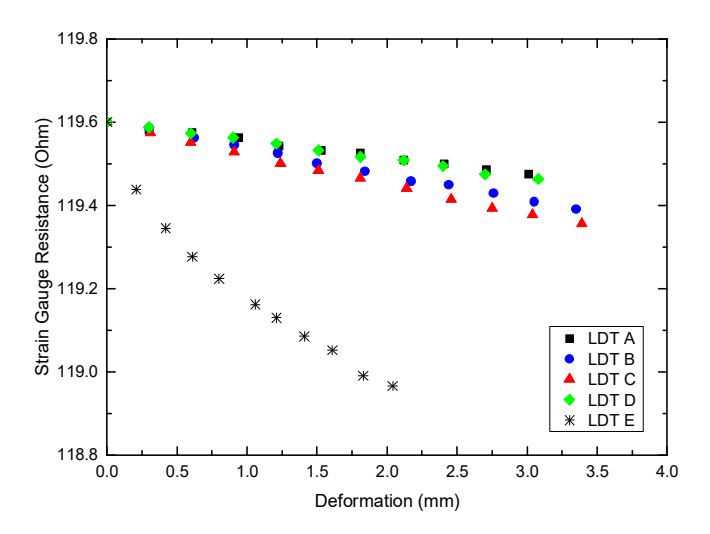


**Figure 9** Relationship between LDT deformation (mm) and resistance changes of the strain gauge ( $\Omega$ ) of the lateral LDTs (A, B, C, D) and the axial LDT (E).

## 5 Repeatability and Stability Tests

Repeatability tests were carried out to evaluate the elasticity performance of the LDTs. This test was required to ensure that the material used as the LDT strip would remain elastic even after it had been deformed many times. In this test, the LDT was forced to deform up to 2.5 mm in 150 second. The force was then reduced at an equivalent time rate until the LDT deformed back to its initial condition. This process was carried out in three repetitions. The repeatability test produced relatively similar relationships between the deformation and the voltage in all repetitions. The average standard deviation against a maximum variation of about 0.2 volt for a maximum deformation of 2.5 mm for LDTs A to D was 0.014 volt, 0.011 volt, 0.023 volt, and 0.013 volt, respectively.

Stability tests were carried out to evaluate the standard error of the LDT system, in which the signal output of the LDT at a fixed position was recorded repetitively (34000 data) for 10 hours. The error produced by this measurement was then evaluated. The standard error is defined as the accuracy of the average value produced by the measurement device. Based on this stability test, the average standard error when the output was about 0.3 to 0.7 volt for LDT A to D was  $2.65 \times 10^{-5}$  volt,  $2.53 \times 10^{-5}$  volt,  $3.2 \times 10^{-5}$  volt,  $2.23 \times 10^{-5}$  volt, respectively. The average standard error of the axial LDT was  $3.13 \times 10^{-5}$  volt.

# 6 Compression Test Program

An unconfined compression test program was conducted to demonstrate the performance of the developed LDT system in actual soil testing. The tests were carried out on three reconstituted natural soil samples in Indonesia, which were classified as clay with high plasticity under USCS. Dealing with natural soil, having the same type of soil does not mean that the characteristics (i.e. soil properties) of each of the sample are necessarily equivalent. The grain size test results of the samples showed that the clay fraction was about 91 to 95% of the samples. The specific gravity was 2.62 to 2.66, and the plasticity index was 18.1 to 26.8. The characteristics of the clay samples are not discussed further since this paper focuses on the demonstration and evaluation of the LDT system. Each of the samples was then prepared as a cylindrical specimen with a diameter of 38.1 mm and a height of 76.2 mm (Figure 10).



Figure 10 Soil specimen instrumented with LDTs.

No saturation and consolidation processes were performed on the specimens in this basic unconfined compression test. As a note, slight inaccuracies were expected in the axial local strain measurements due to the absence of effective confining pressure. Effective confining pressure is required to prevent slipping between the inner face of the membrane and the outer surface of the specimen.

Undrained shearing was conducted to the unconfined specimens at a loading rate of 0.05 mm/min. The axial and lateral deformations of the specimens were measured over a fixed time increment during shearing. As previously mentioned, this test program was designed to observe the performance of the proposed LDT system under very basic compression conditions. The proposed system will be applied to more comprehensive triaxial loadings in another test program referring to the results of this study, as part of the triaxial test apparatus development program at Soil Mechanics Laboratory, ITB, Indonesia.

# **7** Compression Test Results

#### 7.1 Axial and Lateral Deformations

The axial and lateral deformations of the specimens are presented in Figure 11 and Figure 12, respectively. The vertical and horizontal axes of the graphs are the deformation of the specimens in a particular direction and time in the undrained stage, respectively. The time axis can be selected to substitute the load (or stress) working on the specimens since the loading rate was kept constant at 0.05 mm/min. The axial and lateral strains of the specimens were derived from these deformation results, i.e. the change of specimen length (contraction) over its initial length for axial strain, and the change of specimen diameter (expansion) over its initial diameter for lateral strain. Considering the repeatability test results, the maximum axial deformation applied in the soil compression test was set to less than 2.5 mm in order to ensure the elasticity performance of the LDTs.

As shown in Figure 11, the axial deformation of the specimens increased over time due to the increase of the applied load. The results are in the form of scattered data as the output of LDT measurement is a signal. The three specimens exhibited a similar trend of axial deformation behavior, i.e. an increase of deformation due to an increase of constant load over time. Data scattering was relatively low, especially compared to the lateral deformation data discussed above. The measurements show that the first sample may have had uneven soil consistency. This presumption can be pointed out because an erratic deformation pattern was exhibited during loading. On the other hand, the second and the third sample displayed more consistent axial deformation patterns, which could indicate their uniformity in soil consistency.

Different trends can be observed in the lateral deformation pattern in Figure 12. As can be seen in this figure, the lateral deformation of the third specimen increased over time due to the increase of the applied load. However, the first and the second specimen produced slightly different deformation patterns, where the lateral deformation increased to a peak point at about 150 seconds and slightly decreased after that point. This discrepancy may have occurred due to system compliance. The recorded lateral deformation displayed more scattered data than the recorded axial deformation, which is reasonable since (i) more LDTs (i.e. 4) were used to record the lateral deformation measurement (and consequently produced there is more data variation), and (ii) the system boundary is less rigid in the lateral direction (accordingly producing less uniform measurements).

The deformation of the specimens was measured over a time range of 5 minutes. The final readings, as presented in Table 1, were averaged. For comparison, an external sensor system (i.e. linear displacement sensor) was also installed on the cap of the specimens. The axial deformation of the specimens measured by this external sensor system was recorded manually. As can be seen in this table, the axial deformation based on the external sensor was always higher than that based on the LDT. The difference of the measured axial deformation for Specimen 1, Specimen 2, and Specimen 3 was about 18.8%, 16.3%, and 17.2%, respectively. Thus, on average, the external sensor measured axial strains 17.4% higher than the LDT. As a note, Yimsiri, *et al.* [8] observed that the discrepancies between local and external axial strains may range from 30% at very small strains to almost equivalent at larger strains. The discrepancies of these results may have occurred due to the limitations of indirect measurement [3,29].

**Table 1** Summary of the Triaxial specimens' deformation during the final reading.

Triaxial test specimens	Axial deformation (mm)		Lateral deformation (mm)
	LDT measurement	External measurement	LDT measurement
Specimen 1	2.204	2.618	0.046
Specimen 2	1.961	2.281	0.027
Specimen 3	1.668	1.955	0.339

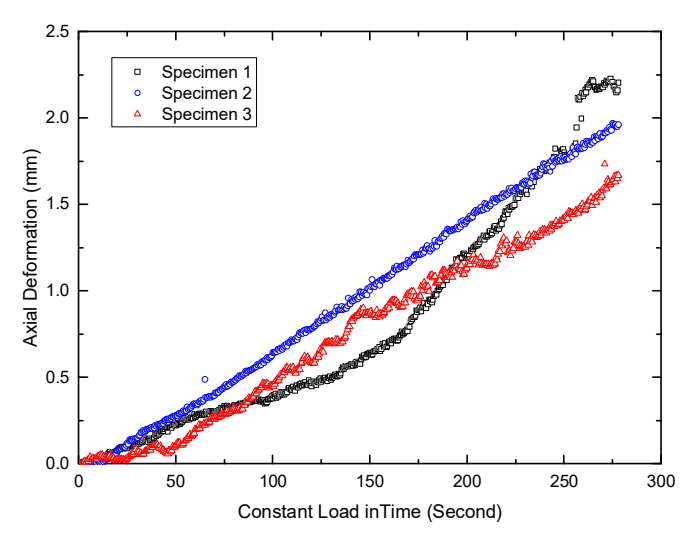


**Figure 11** Axial deformation of the triaxial specimens based on the LDT measurements.

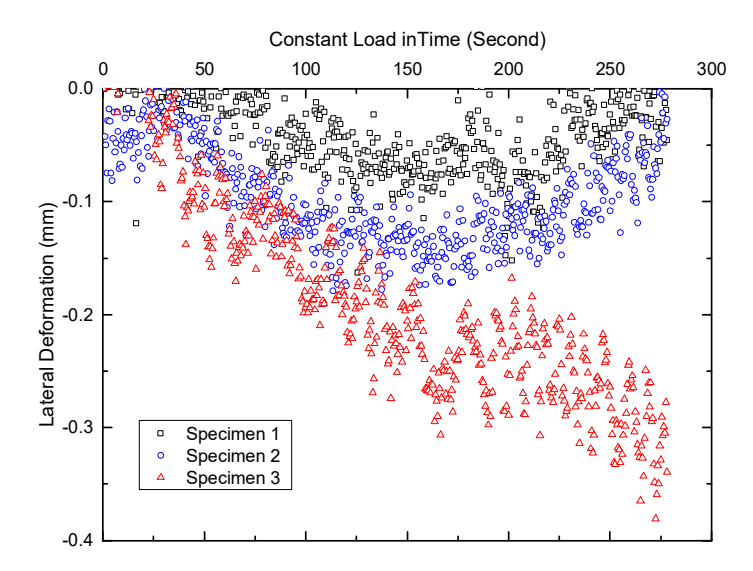


Figure 12 Lateral deformation of the triaxial specimens based on the LDT measurements.

# 7.2 Axial and Lateral Strain Behaviors

The deformation results of the first triaxial test specimen were further analyzed to obtain its strain behavior. The relationship between the axial strain and the lateral strain of the first specimen is presented in Figure 13. The analyzed results were in the form of scattered data. The range of data scattering for the

axial strain and the lateral strain was about 1% and 0.25%, respectively. The data indicate a linear relationship between the axial strain and the lateral strain. It can be observed that the produced lateral strain was smaller than the axial strain at a ratio of about 0.4.

In axial compression tests, the axial deformation is in compression, thus the axial strain is positive. On the other hand, the lateral deformation is tensile, thus the lateral strain is negative. At the end of the measurement, the axial strain ( $\epsilon_a$ ) was about to 2.3% and the lateral strain ( $\epsilon_r$ ) was about -1.0%. This result shows that the specimens exhibited close to zero volumetric strain ( $\epsilon_{vol} = \epsilon_a + 2\epsilon_r$ ), or constant volume behavior, which is reasonable for nearly saturated clay in axial compression.

Curve fitting lines (i.e. linear and polynomial) are presented here to elaborate any exhibited relationship between axial and lateral strain. The linear curve can be represented by the equation y = -0.39x, which is a sensible coefficient considering the undrained shearing that was performed on the specimens. On the other hand, it is interesting to see that the nonlinear curve, represented by a polynomial equation of  $y = -0.66x^2 + 0.15x$ , displayed a better  $R^2$  compare to the linear curve (i.e. 0.97 to 0.94). Considering this result, it can be said that the axial and lateral strain behavior of soils may exhibit a nonlinear association instead of a conventional constant relationship, such as Poisson's ratio.

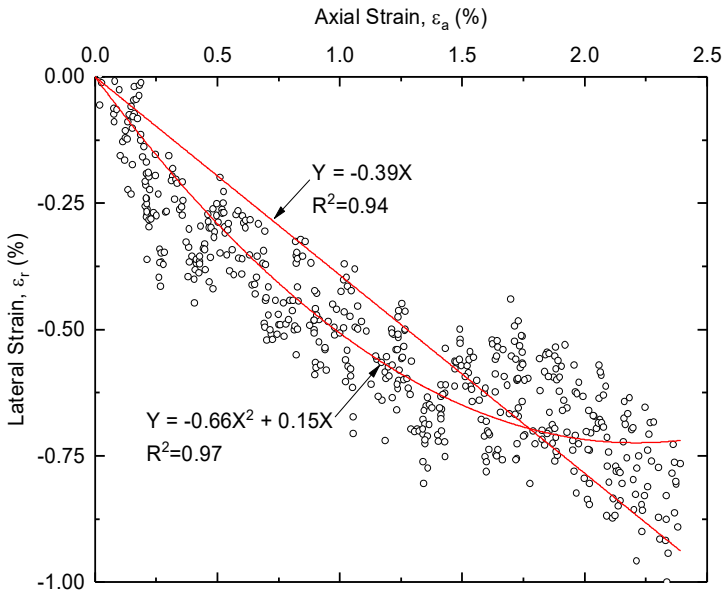


Figure 13 Relationship between axial strain and lateral strain.

## 7.3 Stress-Strain Relationship

Figure 14 presents the relationship between the shear strain and the shear stress of the first specimen. The shear stress is defined as  $(\sigma_1 - \sigma_3)/2$ , where  $\sigma_1$  and  $\sigma_3$  are applied axial pressure and confining pressure, respectively. As previously described, no confining pressure was applied in this test program  $(\sigma_3 = 0)$ . The shear strain was defined as axial strain minus lateral strain  $(\epsilon_a - \epsilon_r)$ . The analyzed results are also presented in the form of scattered data. Unlike the data presented in Figure 13, the range of scattering does not increase to a great extent with straining throughout the curve. This is due to the fact that the curve associates shear strength to a more regular shear stress value, while the previous curve relates axial strain to highly erratic lateral strain data. Yet, the maximum range of scattering occurred at small shear strains, where the range of scattering in the measured shear strain and shear stress were about 0.25% and 80 kN/m², respectively.

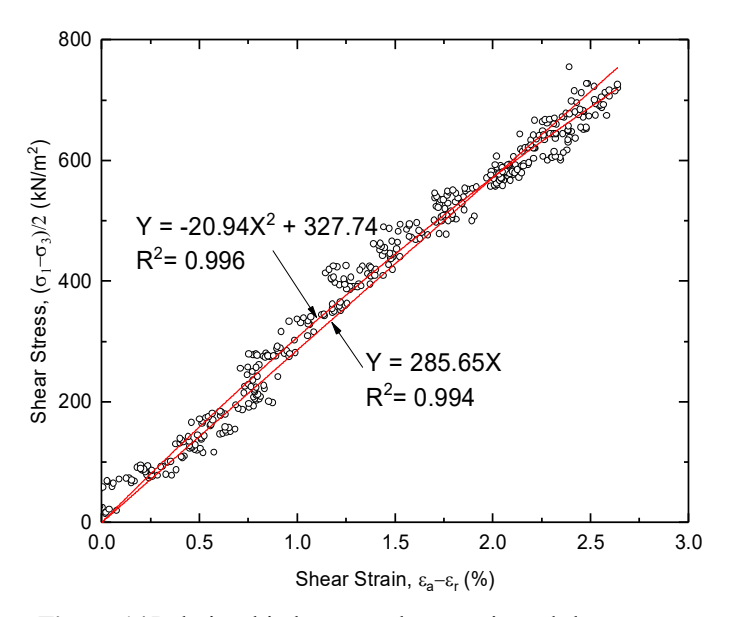


Figure 14 Relationship between shear strain and shear stress.

Like in the previous section, curve fitting lines (i.e. linear and polynomial) are also presented to elaborate the stress-strain behavior of soils. The linear curve can be represented by y = 285.65x, while the nonlinear curve can be represented by  $y = -20.94x^2 + 327.74x$ . Neither peak of shear stress nor strain softening behavior was observed in this axial range, which indicates that the specimen did not reach its plastic yielding and was still in its pre-peak deformation phase. Moreover, it can be observed that the nonlinear curve displays a better  $R^2$  value compared to the linear curve, showing the nonlinear relationship between the

shear strain and the shear stress of soil. This result confirms the previous studies on soil nonlinearity (e.g. [30-32]) and further demonstrates the nonlinear behavior soil exhibits even at small strain levels.

#### 8 Conclusion

An LDT system to locally measure, respectively, axial and lateral strains of a specimen in compression tests was successfully developed. An axial LDT was developed according to the original LDT, while a lateral LDT was developed with a concept similar to the cantilever LDT. Both LDTs were calibrated inside and outside water to evaluate their sensitivity to water inside the triaxial cell. The average difference of the voltage response produced by the LDT's calibration inside and outside the water was about 0.022 volt (for the axial LDT) and 0.021 volt (for the lateral LDT). The calibration factor for the axial and lateral LDTs was 1.695 mm/volt (voltage change of 0.59 volt for every 1 mm LDT deformation) and 1.001 mm/volt (voltage change of 0.999 volt for every 1 mm LDT deformation), respectively. The LDT system was validated by repeatability and stability tests. The repeatability test was carried out to evaluate the elasticity (i.e. the reversibility of deformation) of the LDTs. Furthermore, a stability test was carried out to evaluate the accuracy of the LDT system, which was represented by a standard error value.

A test program was conducted on three reconstituted natural clay samples to demonstrate the performance of the proposed LDT system under basic compression conditions. Curve fitting lines (i.e. linear and polynomial) were presented to elaborate the relationship between the axial and the lateral strain. A nonlinear curve, represented by a polynomial equation of  $y = -0.66x^2 + 0.15x$ , displayed a better  $R^2$  compared to a linear curve (i.e. 0.97 to 0.94), which may indicate the nonlinearity of the axial and lateral strain relationship of soil instead of a conventional constant relationship, such as Poisson's ratio. Furthermore, the stress-strain relationship of the specimen was analyzed. Neither peak of shear stress nor strain softening behavior was observed in this axial range, which indicates that the specimen did not reach its plastic yielding. A nonlinear relationship between shear strain and shear stress, represented by the polynomial equation  $y = -20.94x^2 + 327.74x$ , was exhibited in the results.

The results have confirmed and further demonstrated the nonlinear behavior that soil exhibits even at small strain levels, which was successfully measured using a domestically built axial and lateral LDT system. Future developments can be for example to evaluate the long-term performance of the LDT in cyclic loadings and to apply the system in more comprehensive and advanced soil testing environments. Even though LDT development is globally ubiquitous,

this study is essential to provide a basic platform for the development of experimental soil mechanics in Indonesia.

# References

- [1] Jardine, R.J., Symes, M.J. & Burland, J.B., *The Measurement of Soil Stiffness in the Triaxial App.*, Géotechnique, **34**(3), pp. 323-340, 1984.
- [2] Nakano, R., Shimazaki, F. & Shimizu, H., Anisotropic Mech. Prop. of Diatomaceous Mudstone-with Special Reference to Tensile Young's Mod. and Mech. Prop. of Fault Clay of Tuffaceous Mudstone in Relation to Tunnelung, Proc 7th Jpn. Symp. Rock Mech., pp. 67-72, 1987.
- [3] Goto, S., Tatsuoka, F., Shibuya, S., Kim, Y. & Sato, T., *A Simple Gauge for Local Small Strain Meas. in the Lab.*, SF, **31**(1), pp. 169-180, 1991.
- [4] Burland, J.B. & Symes, M., A Simple Axial Displacement Gauge for use in the Triaxial Apparatus, Géotechnique, **32**(1), pp. 62-65, 1982.
- [5] Clayton, C.R.I., Khatrush, S.A., Bica, A.V.D. & Siddique, A., *The Use of Hall Effect Semiconductors*, Geot. Instrument., **12**(1), pp. 69-76, 1989.
- [6] Clayton, C.R.I. & Khatrush, S.A., A New Device for Measuring Local Axial Strains on Triaxial Spec., Géotechnique, **36**(4), pp. 593-597, 1986.
- [7] Hird, C.C. & Yung, P.C.Y., The Use of Proximity Transducers for Local Strain Measurements in Triaxial Tests, 12(4), pp. 292-296, 1989.
- [8] Yimsiri, S., Soga, K. & Chandler, S.G., Cantilever-Type Local Deformation Transducer for Local Axial Strain Measurement in Triaxial Test, 28(5), pp. 1-7, 2005.
- [9] Cuccovillo, T. & Coop, M.R., *The Measurement of Local Axial Strains in Triaxial Tests using LVDTs*, Géotechnique, **47**(1), pp. 167-171, 1997.
- [10] Ibraim, E. & Benedetto, H.D., New Local System of Measurement of Axial Strains for Triaxial Apparatus Using LVDT, Geotechnical Testing Journal, 28(5), pp. 436-444, 2005.
- [11] Bagherieh, A.R., Habibagahi, G. & Ghahramani, A, A Novel Approach to Measure the Volume Change of Triaxial Soil Samples based on Image Processing, J. Appl. Sci., 8(13), pp. 2387-2395, 2008.
- [12] Ekawita, R., Widiatmoko, E., Nawir, H. & Susila, E., Color Image Processing for Measuring Length Deformation in Compression Test, Proc in 2nd International Conference on Instrumentation, Communications, Information Tech., and Biomedical Eng., 2011.
- [13] Yimsiri, S. & Soga, K., A Review of Local Strain Measurement System for Triaxial Testing of Soils, Geotech Engineering, 33, pp. 43-52, 2002.
- [14] Hongnam, N. & Koseki, J., Quasi-Elastic Def. Prop. of Toyoura Sand in Cyclic Triaxial & Torsional Load., SF, 45(5), pp. 19-37, 2005.
- [15] Kiyota, T., Silva, L.I.N.D., Sato, T. & Koseki, J., Small Strain Deformation Characteristics of Granular Materials in Torsional Shear and Triaxial Tests with Local Deformation Measurements, Proc. Soil

- Stress-Strain Behavior: Measurement, Modeling and Analysis, Springer, Dordrecht, pp. 557-566, 2007.
- [16] Nyunt, T.T., Leong, E.C. & Rahardjo, H., Strength and Small-Strain Stiffness. Characteristic of Unsaturated Sand, Geot. Testing J., **34**(5), pp. 1-11, 2011.
- [17] Tatsuoka, F., Teachavorasinskun, S., Dong, J., Kohata, Y. & Sato, T., Importance of Measuring Local Strains in Cyclic Triaxial Tests on Granular Materials, Proc Dynamic Geotechnical Testing II, 1994.
- [18] Nawir, H., Viscous Effects on Yielding Characteristics of Sand in Triaxial Compression, PhD Dissertation, University of Tokyo, 2002.
- [19] Nawir, H., Tatsuoka, F. & Kuwano, R., Effects of Viscous Prop. on The Shear Yield. Charac. of Sand, Soil & Foundation, 43(6), pp. 33-50, 2003.
- [20] Nawir, H., Tatsuoka, F. & Kuwano, R., Experimental Evaluation of The Viscous Properties of Sand in Shear, SF, 43(6), pp. 13-31, 2003.
- [21] Tatsuoka, F., Nawir, H. & Kuwano, R., A Modelling Procedure for Shear Yielding Characteristics Affected by Viscous Properties of Sand in Triaxial Compression, Soil & Foundation, 44(6), pp. 83-99, 2004.
- [22] Messerklinger, S. & Springman, S.M., Local Radial Displacement Measurements of Soil Specimens in a Triaxial Test Apparatus Using Laser Transducers, Geot. Testing Journal, 30(6), pp. 454-465, 2007.
- [23] Consoli, N.C., Rotta, G.V. & Prietto, P.D.M., *Yielding Compressibility Strength Relationship for An Artificially Cemented Soil Cured under Stress*, Géotechnique, **56**(1), pp. 69-72, 2006.
- [24] Consoli, N.C., Foppa, D., Festugato, L. & Heineck, K.S., *Key Parameters for Strength Control of Artificially Cemented Soils*, J. Geotech. Geoenvironmental Eng., **133**(2), pp. 197-205, 2007.
- [25] Lade, P.V., *Triaxial Testing of Soils*, John Wiley & Sons, 2016.
- [26] Ekawita, R., Munir, M.M., Nawir, H. & Suprijadi, A Comprehensive Characterization of a Linear Deformation Sensor for Applications in Triaxial Compression Tests, Proc in Computer, Control, Informatics and Its Applications (IC3INA), pp. 191-194, 2013.
- [27] Ekawita, R., Development of Measurement System of Sample Dimension on Triaxial Test (in Bahasa), Ph.D. Thesis, ITB, 2015.
- [28] Leong, E.C., Nyunt, T.T. & Low, K.S., *Local Displacement Transducer with Anderson Loop*, ASTM Geot. Testing J., **34**(6), pp. 676-684, 2011.
- [29] Kung, G.T.C., Equipment and Testing Procedures for Small Strain Triaxial Tests, J. Chin. Inst. Eng., **30**(4), pp. 579-591, 2007.
- [30] Viggiani, G. & Atkinson, J.H., Stiffness of Fine-Grained Soil at Very Small Strains, Géotechnique, 45(2), pp. 249-265, 1995.
- [31] Atkinson, J.H., *Non-linear Soil Stiffness in Routine Design*, Géotechnique, **50**(5), pp. 487-508, 2000.
- [32] Clayton, C.R.I. & Heymann, G., Stiffness of Geomaterials at Very Small Strains, Géotechnique, **51**(3), pp. 245-255, 2001.